Available online at www.sciencedirect.com
SCIENCE DIRECT
Coordination Chemistry Reviews 250 (2006) 18–35
COORDINATION CHEMISTRY REVIEWS
www.elsevier.com/locate/ccr

Review

Group 4 metallocene polymerisation catalysts: quantification of ring substituent steric effects

Petra C. Möhring, Neil J. Coville *

Department of Chemistry, Molecular Sciences Institute, School of Chemistry, University of the Witwatersrand, 1 Jan Smuts Ave, Johannesburg 2050, South Africa

Received 1 November 2004; accepted 25 January 2005
Available online 23 February 2005

Contents

Abstract

This review summarises attempts that have been made to *quantify* and separate steric and electronic factors associated with zirconocene-type catalysts in the olefin polymerisation reaction. The use of cone and solid angles, measurement of molecular spaces (coordination gap aperture, obliquity angle and lateral extension angle), the Taft steric parameter as well as a number of theoretical methods (ab initio Hartree Fock, QSAR, 3D-QSAR and paired interacting orbitals) as approaches to the quantification of ligand size is discussed. Attempts to associate these measures with catalyst activity are reviewed.

Keywords: Metallocene; Polymerisation; Catalyst; Steric effect

Abbreviations: cga, co-ordination gap aperture; Cp, cyclopentadienyl ligand, η^5-C_5H_5; Cp^*, pentamethyl cyclopentadienyl ligand, η^5-C_5Me_5; Cp_{cen}, the centroid of a Cp or Ind ligand; CPK, Corey–Pauling–Koltun; Cy, cyclohexyl, $-C_6H_{11}$; DSC, differential scanning calorimetry; EAO, ethylaluminoxane; Et, ethyl, $-CH_2CH_3$; Flu, fluorenyl, η^5-$C_{13}H_8$; Ind, indenyl, η^5-C_9H_7; IR, infra-red; ^{i}Bu, *iso*-butyl, $-CH_2CH(CH_3)_2$; ^{i}Pr, *iso*-propyl, $-CH(CH_3)_2$; ^{n}Bu, *n*-butyl, $-(CH_2)_3CH_3$; ^{n}Pr, *n*-propyl, $-(CH_2)_2CH_3$; MAO, methylaluminoxane; Me, methyl, $-CH_3$; MW, molecular weight; NMR, nuclear magnetic resonance; *p*-Tol, *para*-tolyl; PE, polyethylene; Ph, phenyl; PP, polypropylene; ^{t}Bu, *tert*-butyl, $-C(CH_3)_3$; Bz, benzyl, $-CH_2Ph$

* Corresponding author. Tel.: +27 11 717 6738; fax: +27 11 717 6749.
E-mail address: ncoville@aurum.wits.ac.za (N.J. Coville).

0010-8545/$ – see front matter © 2005 Elsevier B.V. All rights reserved.
doi:10.1016/j.ccr.2005.01.024

1. Introduction

Cyclopentadienyl-containing complexes are one of the most studied groups of organometallic complexes [1]. This is not surprising since Cp–metal complexes can be extremely air and moisture stable, are easily characterised by readily available techniques (IR and NMR spectroscopy, X-ray crystallography etc.) *and* most significantly in the last two decades have played a key role in the development of an understanding of homogeneous catalysis concepts, particularly in the important field of olefin polymerisation catalysis [2].

Complexes of the type Cp_2TiCl_2 were first prepared in the 1950's. Even though they were regarded as excellent models for generating an understanding of the mechanism by which heterogeneous Ziegler-Natta catalysts operated, their actual catalytic olefin polymerization activity was poor [3]. However, the observations by Kaminsky et al. that addition of small amounts of water to the co-catalyst ($AlMe_3$) generated extremely active catalysts, transformed studies in this area of homogeneous catalysis [4].

The initial follow-up studies entailing ligand effects on catalytic activity, by Brintzinger and co-workers [5], Ewen [6] and others, led to an explosion of interest and study in this economically important area of chemistry. Today, many of the principles that lie behind the polymerisation activity of these catalysts are understood and indeed the range of complexes that show olefin polymerisation activity include metals from all parts of the periodic table. Further, many of the newer catalysts no longer contain cyclopentadienyl or related ligands (e.g. indenyl rings) as the role of the ligand in the reaction mechanism, in terms of steric and electronic effects, can readily be transferred to all ligand types. Significantly, the newest range of homogeneous Ti containing catalysts, centered on a 6-coordinate site, may provide the best model for understanding the heterogeneous Ziegler-Natta catalysts [7].

Our own interest in this arena commenced initially from issues unrelated to homogeneous catalysis. For some years we had been exploring the role of catalysts in the *synthesis* of organometallic complexes [8]. In these studies we had noted that $[(CpR)Fe(CO)_2]_2$ complexes were efficient catalysts for simple substitution reactions, e.g.

$$CpFe(CO)_2I + PPh_3 \rightarrow CpFeCO(PPh_3)I + CO \quad (1)$$

As an outgrowth of this study, and to investigate the reaction mechanism, we commenced a study of the synthesis of a range of (CpR)Fe(CO)LI complexes (R, L – variable groups) and to our surprise found that features of the NMR spectra of the cyclopentadienyl ring protons correlated with the cone angle of L (e.g. phosphine) [9]. The results qualitatively suggested that the ring was sterically interacting with the L group and prompted us to seek procedures that would allow us to quantify the size of the cyclopentadienyl ring. This naturally set us on a path to seek methods to quantify ligands in terms of size. The outcome was our development of various measures (cone angles, solid angle measurements, ligand profiles etc.) for measuring the size of substituted cyclopentadienyl ligands [10].

It was at this time that the study of the olefin polymerisation performance of the Cp_2ZrCl_2 catalyst precursors was in its 'heyday'. One of the keys to the success of metallocenes in olefin polymerisation was the ability to manipulate activity, molecular weight, co-monomer incorporation, and stereospecificity by choice of Cp ring substituents. The elucidation of ligand effects, leading to rational ligand design at the transition metal center, has been central in the development of metallocene technology over the past two decades. Even one substituent is sufficient to introduce novel features into catalytic behaviour, stability and reactivity of metallocene complexes.

In an attempt to establish the role of steric effects in the new metallocene catalysts, we applied our steric measures to these new cyclopentadienyl-containing polymerisation catalysts. In particular we wished to establish whether it was possible to separate and quantify the steric and electronic effects of ring substituents on catalyst activity [11,12]. This attempt to categorise and relate ligand properties to catalytic properties is intuitively appealing (even though it may oversimplify the problem). By associating some readily available 'number' with a ligand it is then possible to systematically vary ligands in a reaction and relate activity effects to easily understood concepts associated with a ligand (size, electron withdrawing- or donating ability).

This approach has been used to evaluate the role of phosphines in many catalytic reactions, a tradition that is still carried on today. Indeed, *all* organometallic chemistry textbooks introduce phosphine/phosphite steric effects via the Tolman cone angle, and indicate that some understanding of reactivity patterns using organometallic catalysts can be obtained from this measure [13,14]. What of steric and electronic measures for cyclopentadienyl and related ligands? In the mid-1990's we [11,12,15–18] and others [19–21] have made attempts to quantify and separate steric and electronic factors associated with zirconocene-type catalysts in the olefin polymerisation reaction with catalyst activity using a similar philosophy.

Below we have brought together the older and newer results on this issue and have indicated the current status in the field. We have only evaluated literature reports in which some attempt at associating the *quantification* of steric (or steric and electronic) effects with catalyst activity has been made. We have divided the discussion into sections that relate to the different measures currently used in the field. In each instance we have firstly given an overview of the methodology used and then indicated the catalytic studies in which it has been applied.

This review covers research in olefin polymerisation by metallocene catalysts published before mid-2004. While metallocenes are generally defined as metal complexes with two Cp rings, this review will additionally cover catalysts containing only one Cp ring, as well as catalysts with ligands isolobal to the cyclopentadiene ligand.

2. Polymerisation activity and steric and/or electronic substituent effects – general issues

It has long been realised that the steric and electronic parameters of a particular ligand cannot be viewed in isolation and it is usually a combination of the two effects that can be correlated with the properties and behaviour of a compound. Tolman proposed the use of a multivariate approach where a measurable parameter Z could be analysed with respect to both steric and electronic parameters according to Eq. (2):

$$Z = a\theta + b\nu + c \tag{2}$$

where θ is the steric parameter, ν an electronic contribution and a, b and c are the regression coefficients [14]. The percentage contribution of the steric effect could then be determined using Eq. (3):

$$\text{steric effect}\,(\%) = \frac{a}{a+b} \times 100 \tag{3}$$

It is this approach that is generally assumed to hold in all studies that have been reported subsequent to the original Tolman papers. (Alternative proposals have since been made; see below.)

Prior to describing how this approach has been applied to zirconocene-type polymerisation catalysts, it is worth noting that differing reaction conditions can overwhelm any comparative data that relate to the ligand effects. Over the years numerous comments have been made in the literature that relate to the effect of variables that affect catalyst polymerisation behaviour. Indeed, examples of different activity series for the *same catalysts* have been reported in the literature [11,18,22,23]. Comparison of data between different researchers is made difficult since the studies usually involve different experimental conditions such as reagent purity, catalyst concentration, Al:Zr ratio, temperature, monomer pressure, MAO characteristics, etc. [22]. Some of these variables are highlighted below.

Reaction conditions employed during a polymerisation reaction can affect the ordering of activities by influencing reaction equilibria of reactants and intermediates (e.g. ion pairs) as shown in Fig. 1 [24]. Only separated ion pairs can insert olefin molecules, whereas the non-separated species may be regarded as dormant and incapable of contributing to polymer growth. The effect of these equilibria is particularly important in cases where the steric and electronic properties of the complexes are quite similar.

The *choice of monomer* (and co-monomer) is important. Ethylene is typically the monomer of choice for comparative studies as it limits stereochemical issues. It has been observed in propene studies that the stereospecificity of the catalyst also strongly affects the activity and is thereby able to overcompensate electronic and steric influences [22,25,26].

The *range of ring substituents* that have been investigated limits the range of steric and electronic effects accessible for study. As a wider range of substituents are attached to the ring, so the degree of confidence in a quantitative measure will increase [27].

The *catalyst concentration* has a dramatic effect on relative polymerisation activities. At high concentrations, polyethylene precipitates rapidly, especially for more active catalysts. The polymerisation is then truly homogeneous only in the very beginning of the reaction, after which the active complex becomes embedded in the polymer matrix, leading to a diffusion-controlled polymerisation reaction. Thus the electronic or steric effects of the catalysts can no longer be compared. Only the initial rate in the first few seconds of the reaction should correspond to a characteristic rate for the homogeneous catalyst and reflect the electronic and steric variations. It is, however, difficult to monitor these initial rates [24,28] (particularly in the case of highly active MAO-activated zirconocene systems), or to extrapolate the rates to time = 0.

The increase in activity with increasing Al:Zr ratio and decreasing Zr concentration can also influence the results. This effect arises from (i) a later precipitation of polymer together with the change to the diffusion-controlled rate limit, such that in diluted solutions the homogeneous complex with its higher activity dominates the polymerisation profile [29] and (ii) the known "infinite" increase in activity with the increase of the Al:Zr ratio [6b,30–32]. The same Al:Zr ratio can also lead to a different equilibrium position between the catalyst and the MAO co-catalyst, i.e. to a different relative concentration of the active species, for different catalysts [29]. This effect is, of course, also a consequence of the differences in the steric and electronic requirements of the complexes. Since the full functionality of MAO and most importantly its interaction with or its role in the activated metallocene is not known [33], it is, not currently possible to judge the relative effects.

Irreversible *catalyst deactivation* may also influence catalyst performance as ligands are varied since the stability of these complexes is presumed to be affected by their ligand structure [22].

Finally, relationships between catalyst steric and electronic factors may be *non-linear*. However, in most cases insufficient data exists to test for higher-order relationships and interactions between effects.

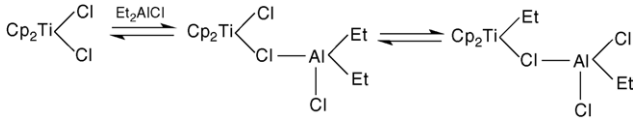

Fig. 1. Reaction between metallocene and alkylaluminium species showing the conversion between Lewis acid–base and dissociated ion pairs.

3. Approaches to the quantification of substituent steric effects in group 4 metallocene polymerisation catalysts

The different approaches are discussed in (roughly) chronological order of their use in this area of chemistry.

Table 1
Steric measurements for η^5-$C_5H_{5-n}R_n$ ($n = 1$ unless otherwise indicated)

R	θ_1 (°)[a]	θ_1 (°)[b]	θ_1 (°)[c]	θ_1 (°)[d]	θ_2 (°)[e]	Ω_{av} (°)[f]	Ω_A (°)[g]	Ω_N (°)[h]	cga (°) $(CpR)CpZrCl_2$[i]	cga (°) $(CpR)_2ZrCl_2$[i]	cga (°) $(CpR)_2ZrCl_2$[j]	E_S^0[k]
H	128	116	135	139	56	131	117	120	92	92	96	0
	148								95[l]			
	150[m]											
Me	141	128	140		64	144	122	125			91	−0.25
Me, $n = 2$						157						
Me, $n = 3$						167						
Me, $n = 4$				164		177			76	62		
Me, $n = 5$	182			171		187			75	55		−3.85
	188[d]											
Et	146	132	143		85	150	126	129			87	
^{n}Pr	178				172							
^{i}Pr	150	135	143		107	156	128	130			86	−1.1
^{i}Pr, $n = 2$												−2.2
^{n}Bu												−1.9
^{i}Bu												−1.78
^{t}Bu	154	139	148	156	128	164	133	135	74	58	81	−2.39
1,3-^{t}Bu$_2$				173					66	40		
1,2,4-^{t}Bu$_3$				190					54.5			
$SiMe_3$	158	144	146		138	161	131	134			85	−3.7
Cy												−1.44
Cy, $n = 2$												−2.88
$CH{=}CH_2$	151				39							
$CH_2CH{=}CH_2$												
CH_2Ph	150		146		102	182	129	131			81	
$CHPh_2$	158				140	192						
CMe_2Ph	158	145	147		144	172	136	136			83	
$CMePh_2$	163				161	180						
CPh_3	167				178	191						
Ph	133				71	144						
F						133						
Cl						134						
Br						135						
I						135						
SH						132						
SMe	154				122	139						
OMe	155				132							
NH_2	141				64	138						
NHMe						150						
NMe_2	154				131	158						
NEt_2	176				174							
NO_2	142				60	141						
COMe	142				47	144						
CO_2Me	132				47	141						
PMe_3	159				143							
PPh_3	170				149							
η^5-C_4Me_4P				167					75	58		

[a] Ref. [38]; measured from the metal as apex, based on Fe system with centroid–Fe distance of 1.73 Å.
[b] Ref. [12]; based on Zr system with centroid–Zr distance of 2.2 Å.
[c] Ref. [18]; based on Zr system using the centroid–Zr distance for the corresponding $(CpR)_2ZrCl_2$ complexes.
[d] Ref. [19]; see paper for details of bond lengths used.
[e] Ref. [38]; measured from the perspective of the ring centroid.
[f] Ref. [41]; solid angle measured from Fe with centroid–Fe distance of 1.73 Å.
[g] Ref. [75]; solid angle calculated using analytical method.
[h] Ref. [40]; solid angle calculated using numerical method.
[i] Ref. [19]; co-ordination gap aperture.
[j] Ref. [20,21].
[k] Ref. [64]; Pal'm steric parameter.
[l] Ref. [21].
[m] Ref. [37]; values for Rh^I and Rh^{III} complexes.

Table 2
Steric measurements for 1- and 2-substituted (R-Ind)Zr fragments[a]

1-R	2-R	θ_1 (°)[b]	Ω_N (°)[c]	Ω_A (°)[d]
H		143	127	123
Me		150	135	130
	Me	150	135	131
Et		149	136	133
	Et	149	136	131
^{i}Pr		152	138	134
^{t}Bu		163	147	144
$SiMe_3$		163	147	144
	$SiMe_3$	164	148	144
Ph		152	139	134
	Ph	150	139	134
Bz		149	136	132
	Bz	149	136	133
(1)-Napth		152	139	133
	(1)-Napth	150	140	136

[a] Measured from the metal as apex, based on Zr system with centroid–Zr distance of 2.239 Å [17].
[b] The Tolman cone angle [13,14].
[c] Solid angle calculated using numerical method [40].
[d] Solid angle calculated using analytical method [75].

A listing of calculated steric measures for substituted metallocene complexes, that have been reported, is given in Tables 1–4.

Table 3
Steric measurements for bridged Cp complexes[a]

Complex	cga (°)
Me_2Si(2-Me,4-Ph-C_5H_2)$_2ZrCl_2$	91
Me_2Si(2-Me,4-^{t}Bu-C_5H_2)$_2ZrCl_2$	79
C_2H_4(2-Me,4-Ph-C_5H_2)$_2ZrCl_2$	97
C_2H_4(2-Me,4-^{t}Bu-C_5H_2)$_2ZrCl_2$	70

[a] Ref. [20].

3.1. Cone angle and solid angle

3.1.1. Cone angle methodology

The cone angle concept was originally proposed by Tolman [13,14]. The Tolman cone angle, θ, is the sum of the half-vertex angles for n unsymmetrical groups in a ligand, multiplied by two (Fig. 2 and Eq. (4)).

$$\theta = \frac{2}{n}\sum_{i=1}^{n}\frac{\theta_i}{2} \quad (4)$$

Cone angles were initially generated for a series of phosphines and phosphites, L, to rationalise catalytic studies involving $Ni(CO)_3L$ and these data have since provided a relative ordering of size that can be generalised to any atom or substituent [10]. Some typical cone angles values for phosphine and phosphite ligands are provided in Table 5.

Table 4
Geometrical data for selected $(CpR)_2ZrCl_2$ derivatives[a]

	α (°)[b]	β (°)[c]	γ (°)[d]	τ (°)[e]	ϕ (°)[f]	$\Delta(d_{Zr\text{-}C})$ (Å)[g]
Unbridged						
Cp_2ZrCl_2	53.5	126.5	129.2	1.4	–	0.041
$(CpMe_4)_2ZrCl_2$	53.6	126.4	133.3	3.45	–	0.118
$(CpMe_5)_2ZrCl_2$	43.7	136.3	130.9	−2.7	–	0.067
$(CpMe_4Et)_2ZrCl_2$	43.8	136.2	137.0	0.4	–	0.036
Single bridges						
$[H_2C(C_5H_4)_2]ZrCl_2$	70.0	110.0	116.4	3.2	16.3	0.104
$[H_2C(C_5H_4)_2]ZrI_2$	70.8	109.2	116.6	3.7	15.7	0.114
$[Me_2C(C_5H_4)_2]ZrCl_2$	71.4	108.6	116.6	4.0	14.9	0.118
$[(CH_2CH_2)(C_5H_4)_2]ZrCl_2$	56.4	123.6	125.8	1.1	4.3	0.053
$[(Me_2CMe_2C)(C_5H_4)_2]ZrCl_2$	57.4	122.6	125.0	1.2	3.0	0.048
$[(CH_2CH_2)(C_5Me_4)_2]ZrCl_2$	57.7	122.3	127.7	2.6	1.3	0.095
$[(CH_2CH_2CH_2)(C_5H_4)_2]ZrCl_2$	50.2	129.8	129.6	−0.1	7.0	0.027
$[Me_2Si(C_5H_4)_2]ZrCl_2$	60.1	119.9	125.4	2.8	16.6	0.074
$[Me_2Si(C_5Me_4)_2]ZrCl_2$	60.8	119.2	128.6	4.7	17.8	0.149
$[(Me_2SiMe_2Si)(C_5H_4)_2]ZrCl_2$	51.2	128.8	130.9	1.05	0.5	0.031
$[(Me_2SiMe_2Si)(C_5Me_4)_2]ZrCl_2$	50.3	129.7	136.1	3.2	−13.4	0.095
$[(Me_2SiOMe_2Si)(C_5H_4)_2]ZrCl_2$	51.1	128.9	130.8	0.95	5.1	0.036
Double bridges						
$[\{(CH_2CH_2)_2\}(C_5H_3)_2]ZrCl_2$	62.5	117.5	120.0	1.25	1.7	0.052
$[(Me_2Si)_2(C_5H_3)_2]ZrCl_2$	69.6	110.4	120.6	5.1	19.6	0.157

[a] Ref. [54a] and references therein.
[b] α = Interplanar ring angle.
[c] $\beta = Cp_{norm}–Cp_{norm}$ angle ($\alpha + \beta = 180°$).
[d] $\gamma = Cp_{centroid}–M–Cp_{centroid}$ angle.
[e] $\tau = 0.5(\gamma–\beta)$ = tilt angle (the angle between the M-$Cp_{centroid}$ vector and the ring normal).
[f] $\phi = 180° - (A - C_{ipso} - Cp_{centroid})$, the angle between the $A - C_{ipso}$ vector and the Cp mean plane.
[g] variation in Zr─C bond lengths.

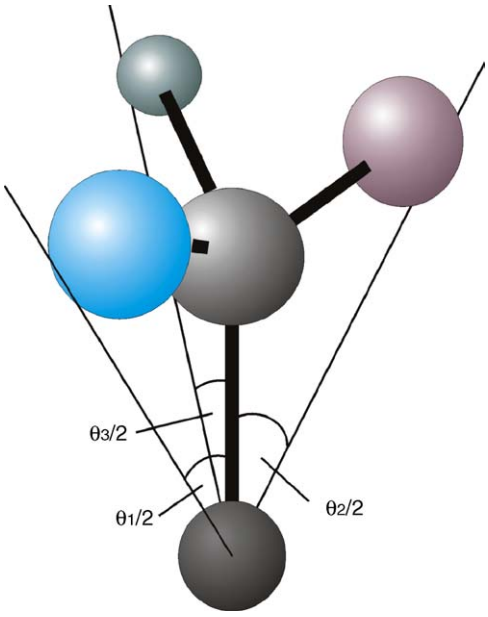

Fig. 2. The Tolman cone angle methodology involves the measurement of the half-vertex angle, $\theta/2$, for each substituent in an unsymmetrical ligand. Figure was reproduced from Ref. [36], with permission of the copyright holders.

Table 5
Cone angles for selected phosphine and phosphite ligands[a]

Ligand	θ (Tolman cone angle) (°)
Phosphine ligands	
PH_3	87
PMe_3	118
PEt_3	132
$P(^nPr)_3$	132
$P(^nBu)_3$	132
$P(^iBu)_3$	143
$P(^tBu)_3$	182
Phosphite ligands	
$P(OMe)_3$	107
$P(OEt)_3$	109
$P(O^iPr)_3$	130
$P(O^nBu)_3$	110

[a] Ref. [10].

Poë has pointed out that values of θ, with minor exceptions, are still those provided by Tolman [14] in spite of the absence of an understanding of why the relatively crude methodology used to derive cone angles should be so successful [34]. The reason for the continued use of Tolman's cone angles is that their use is successful, i.e. they allow a quantitative description of the dependence of many diverse physicochemical properties on the electronic and steric natures of the ligands involved. Poë has argued that a better approach to the use of Tolman cone angles would be to use them as a starting point in analysing electronic and steric effects, but then allow for their adjustment by repeated tests of their 'goodness of fit' to a large number of data sets when they are treated as variables. This process assumes, in the first instance, that the electronic parameters that are used are essentially correct and the cone angles are then determined by the need for their values to provide the best possible fits of a wide range of data to the appropriate equations. Subsequently, for ligands with reliable cone angles, but dubious electronic parameters, the electronic parameters can then be refined. Such an iterative process would be similar to that used by Fernandez et al. [35] for a restricted set of ligands.

In the Tolman cone angle calculation for a substituted Cp ligand, the half-vertex angle to each of the five Cp carbon atom substituents is measured [36]. It is also possible to measure the cone angle from the ring centre. While Maitlis first used the Tolman concept to measure cone angles for substituted Cp rhodium complexes [37], Coville et al. were the first to use both procedures to measure cone angles for monosubstituted Cp complexes [38] (Fig. 3).

3.1.1.1. With metal as apex (θ_1) (Fig. 3(a)). The general procedure used here is to calculate the size of a cone which will encompass the ligand with the metal as the apex, as performed for PR_3 ligands. This method takes into account the degree of substitution of the ring. Since free rotation of the Cp ring about the metal–$Cp_{centroid}$ axis takes place in solution [39], the alkyl group R occupies one of the five ring positions only 20% of the time. Thus, for an n-substituted ring, $C_5R_nH_{5-n}$, the average cone angle is given by

$$\theta_1 = \frac{5-n}{5}\alpha + \frac{n}{5}\beta \quad (5)$$

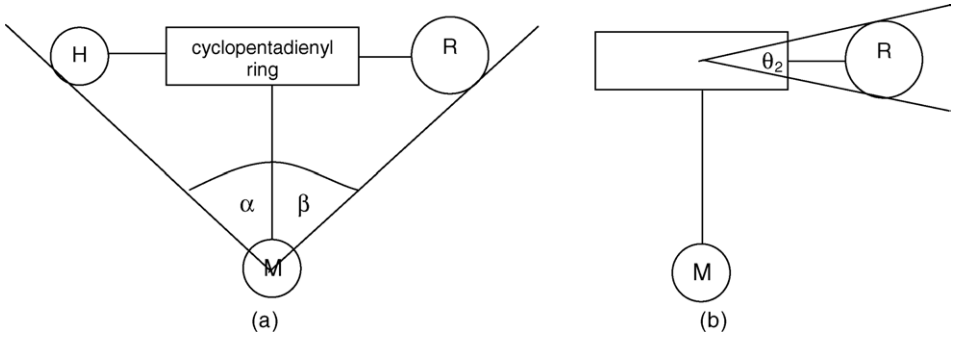

Fig. 3. Measurement of the average cone angle, θ, for a substituted Cp ring. (a) The measurement of θ_1 (metal as apex of the cone). (b) The measurement of θ_2 (ring centroid as apex of the cone).

where α is the cone angle for C_5H_5 and β the cone angle for C_5R_5.[1] Initially, calculations were based on a metal–$Cp_{centroid}$ distance of 1.73 Å, corresponding to the average Fe-ring centroid distance for a range of (CpR)Fe(CO)(L)I complexes [38]. Later, a metal–$Cp_{centroid}$ distance of 2.2 Å was chosen to generate the cone, a value consistent with crystal structure data for Cp–zirconium complexes [12]. These calculations were further refined by using the actual zirconium–$Cp_{centroid}$ distances (from crystal structure data) for each complex under consideration [18]. Using this method, the cone angles for C_5H_5, C_5H_4Me, C_5Me_5 and $C_5H_4{}^tBu$ ligands are 128°, 141°, 182° and 154°, respectively.

3.1.1.2. With ring centroid as apex (θ_2) (Fig. 3(b)). In this method, the ring centroid is chosen as apex for a cone, which includes the ligand groups. Thus, a mean plane through the Cp ring carbons is defined and the angle between the vector tangential to the van der Waals radius of the outermost atom and its projection in the plane is calculated. This measure does not distinguish between different degrees of Cp ring substitution. Using this method, the cone angles for C_5H_5, C_5H_4Me, C_5Me_5 and $C_5H_4{}^tBu$ ligands are 56°, 64°, 64° and 128°, respectively.

3.1.2. Solid angle methodology

First efforts to develop the quantification of steric effects by means of solid angles involved the detection of steric effects using molecular mechanics to produce ligand profiles, while later methods focused on the quantification of the solid angles [10].

The analytical solid angle, Ω_A is defined as the surface area of that part of a solid projected onto the surface of a unit sphere (Fig. 4). The equation for calculating the solid angle, Ω, is defined by the integral given in Eq. (6).

$$\Omega = \int_s \frac{r\,\mathrm{d}S}{r^3} \tag{6}$$

The analytical solid angle is calculated in the integrand by subtending a vector **r** (whose magnitude is r) from an origin position to a point on a surface, whose area is dS. If the ligand shadow covers the entire sphere, the solid angle will be 4π steradians (sr). Steradians are not the unit of choice for expressing the size of a ligand. Conversion to the angle of a cone, which covers the same area, allows this measurement to be expressed in degrees (Eq. (7)).

$$\theta(^\circ) = 2\ \arccos\left[1 - \frac{\Omega\,(\mathrm{sr})}{2\pi}\right] \tag{7}$$

This analytical solid angle calculation takes into account the actual shape of the group of atoms under investigation, but is problematic in accounting for overlap between atoms. Using this method, the cone angles for C_5H_5, C_5H_4Me and $C_5H_4{}^tBu$ ligands are 117°, 122° and 133°, respectively.

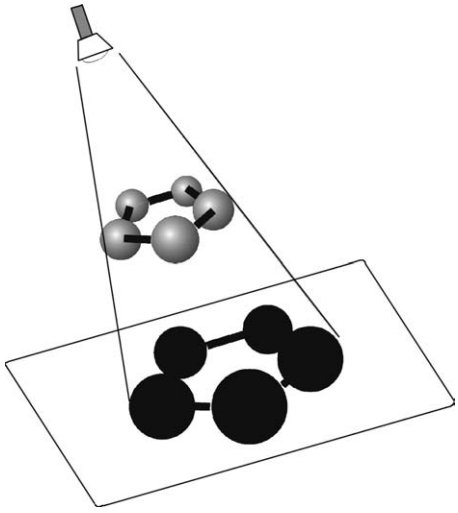

Fig. 4. The analytical solid angle is calculated by reflecting the shape of the ligand onto a unit sphere and calculating the size of the shadow. Figure was reproduced from Ref. [36], with permission of the copyright holders.

The numerical solid angle, Ω_N, can be considered as a compromise between θ and Ω measurements [40]. In this calculation, a *non-circular cone* is traced around the outer van der Waals radius of the ligand being measured. This cone is measured by rotating an axis through Φ degrees, thereby measuring the semi-cone angle, $\theta/2$, around the group being studied (Fig. 5 and Eq. (8)). The values derived from this calculation can be converted into the angle of a cone using Eq. (7).

$$\Omega_N = \int_{\phi=0}^{2\pi} \left(1 - \cos\frac{1}{2}\theta\right) \mathrm{d}\phi \tag{8}$$

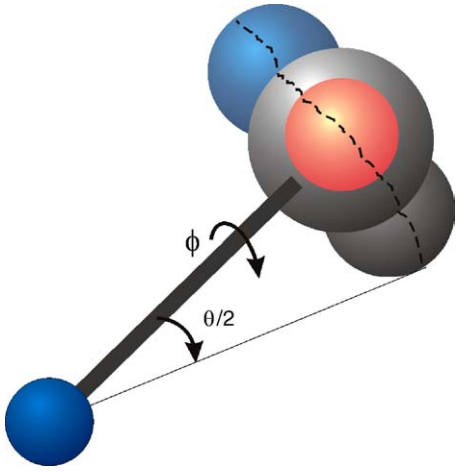

Fig. 5. Representation of the ligand angular profile used to create a non-circular cone. Figure was reproduced from Ref. [36], with permission of the copyright holders.

[1] For example, for the C_5Me_4H ring, $\alpha = 139°$ (for C_5H_5), $\beta = 171°$ (for C_5Me_5), $n = 4$ and thus $\theta_1 = 164°$.

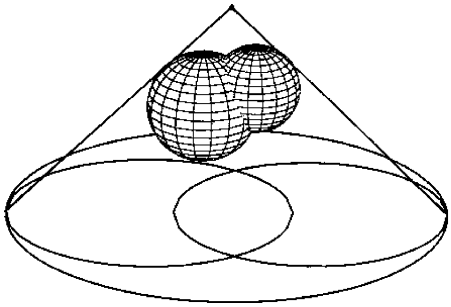

Fig. 6. Projection of two spheres onto the base of an enveloping cone to form two ellipses. The unused portion of the enveloping cone is subtracted by integration leaving the solid angle of the two ellipses.

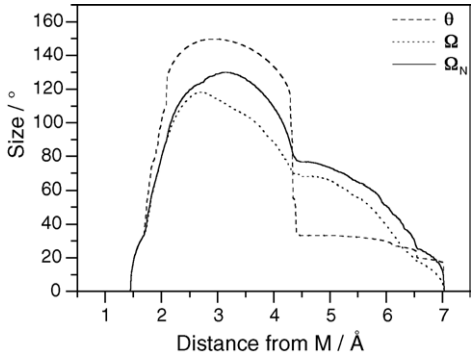

Fig. 7. Ligand profile plots for a ^{t}Bu-Cp ligand positioned 2.202 Å from the point of measurement. Figure was reproduced from ref. [36], with permission of the copyright holders.

Using this method, the cone angles for C_5H_5, C_5H_4Me and $C_5H_4{}^tBu$ ligands are 120°, 125° and 135°, respectively (see Table 1 for more data).

An analytical, simplifying, approach to this calculation was developed by White et al. [41] and Taverner [42]: the calculation is started by considering only a pair of atoms bound together with the required overlap between their atomic radii. An enveloping cone is placed around these atoms, which are projected onto the base of the cone (Fig. 6). The total solid angle of the cone is trivial to calculate. To obtain the solid angle for a group of many atoms, the individual atoms in the molecule are traversed in pairs, subtracting the relevant portions added more than once.

This approach is general, i.e. it is applicable to any atom or combination of atoms in any geometrical arrangement in space. It provides a measurement in units, which are intuitively meaningful to chemists and can be generated from a knowledge only of bond lengths, bond angles and atomic radii. The method also takes into account group meshing. Solid angle calculations have been used to quantify the size and shape of Cp ring substituents [41,43] as well as indenyl ring substituents [17].

Calculation of cone angles as well as numerical and analytical solid angles was carried out for $(CpR)_2ZrCl_2$ complexes: (1) with all the Zr–C_{Cp} bond distances the same and (2) with bond lengths as given by X-ray crystallographic data. The two sets of results were very similar, indicating that ring-tilt in these complexes can be ignored [18]. The same assumption was made for the related indenyl complexes [17].

The numerical and analytical solid angle measurements are considered an improvement over the Tolman cone angle as the latter assumes *cylindrical* symmetry of the ligand and ignores spaces between the atoms of the ligand. The Tolman cone angle, numerical and analytical solid angle calculations can also be used in the measurement of ligand profiles. Here the size of the ligand is measured as a function of the distance from the point of measurement (Fig. 7) [10,36,44].

3.1.3. Applications

Cone and solid angles, together with Hammett substituent constants [45] have been used to measure (and separate) steric and electronic parameters associated with substituted Cp rings [11,12,15–18]. The advantages of this approach are that (i) both are expected to be pure measures of their respective parameters, which permits separation of steric and electronic effects [46], (ii) both are quantitative measures, thus allowing statistical analysis of correlation to be performed, (iii) both have values for a wide range of substituents and (iv) both are universal measures, i.e. the values are independent of the metal centre or the type of complex under investigation.

In all the studies reported [12,16–18], the reactions were carried out at low Zr concentrations (1.04×10^{-7} to 6.25×10^{-6} M) and high Al/Zr molar ratios (30,000–64,000). Conditions were selected to avoid the precipitation of polymer during the reaction, thus minimising the influence of diffusion-controlling processes in which the polymerisation reaction may become heterogeneous in nature. The polymer was produced at an initial high rate of ethylene uptake followed by a lowered product yield as the catalyst deactivated. The effect of the different ligands on the kinetics and equilibria of active site formation (as discussed in Ref. [24]) were not studied; instead an attempt was made to associate ground state effects with polymerisation activity. Note also that in these studies, the relative contribution of the steric and electronic effects was determined according to Eq. (3), but with each coefficient first multiplied by the range of the corresponding parameter.

In a study of the ethylene polymerisation behaviour of a series of $(CpR)_2ZrCl_2$/EAO catalysts (R = H, Me, Et, ^{i}Pr, ^{t}Bu, $SiMe_3$ and CMe_2Ph) [12], the best fit to the data was obtained by using θ_2 (the cone angle with ring centroid as apex) and the Hammett substituent parameter, F, which is a linear combination of the more well-known substituent constants σ_m and σ_p [45] (Fig. 8). Re-analysis of the data has shown that 78% of the variation in the data can be explained by the model, which is significant at the 95% confidence level ($p = 0.02$) [47]. Use of any steric or electronic parameter alone did not explain a sufficiently high proportion of the variance in the data; a linear combination of both a steric and electronic parameter was required. An increase in ligand size resulted in a small increase in activity (32% of the total effect as defined in Eq. (3)) thought to be associated with stabilisation of

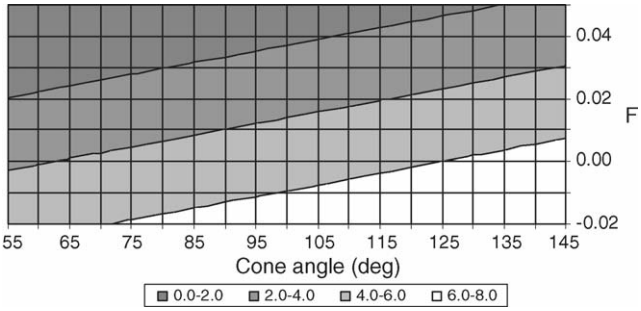

Fig. 8. Contour plot of activity data [12] vs. the cone angle, θ_2, and the electronic parameter, F. The surface represents the least-squares fit to the data given by the equation: activity ($\times 10^5$ g PE mol Zr^{-1} h^{-1}) = $0.032(\theta_2) - 85.6(F) + 1.99$.

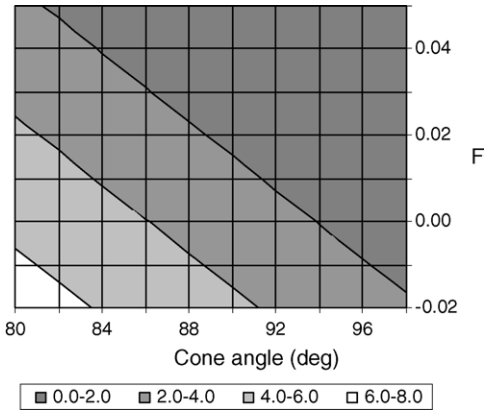

Fig. 9. Contour plot of difference in activity data between homo- and copolymerisation reactions [16] vs. the cga and the electronic parameter, F. The surface represents the least-squares fit to the data given by the equation: activity difference ($\times 10^5$ g PE mol Zr^{-1} h^{-1}) = $-0.26(\text{cga}) - 65.6(F) + 26.4$.

the active site (by larger ligands) against deactivation by bimolecular disproportionation. An increase in ligand electron donating ability produced a large increase in polymerisation activity (68% of the total activity change). Electron-donating substituents are thought to decrease the positive charge on the metal centre, weaken the bond between the metal and its ligands, hence destabilising the metal–alkyl bond, thus increasing catalytic activity.

Similar results are obtained for this data set when θ_2 is replaced by the coordination gap aperture [19,22] (77% of the variation in the data is explained by the model; $p = 0.02$). The steric effect contributes 40% of the total effect and the electronic effect 60%. The use of solid angles gave similar models, but accounted for a lower degree of variance.

In a related study on the ethylene/1-hexene copolymerisation behaviour of a series of $(CpR)_2ZrCl_2$/EAO catalysts (R = H, Me, Et, ^{i}Pr, ^{t}Bu, $SiMe_3$ and CMe_2Ph) [16] it was found that the copolymerisation activities could not be explained by a linear combination of steric (cone angle, solid angle or cga) and electronic parameters as described above. However, a moderate correlation was obtained between the *difference* between the co- and homopolymerisation activities and a linear combination of the coordination gap aperture [19,22] and the electronic parameter, F (Fig. 9). Re-analysis of the data showed that 69% of the variation in the data could be explained by the model, which was significant at the 95% confidence level ($p = 0.04$) [47]. The overall activity difference change was related almost equally to steric (46%) and electronic (54%) effects. The difference in activity increases (i.e. relative copolymerisation ability decreases) as the steric bulk of catalyst increases (due to increased steric hindrance to the approach of 1-hexene to the active site) and as the electron-donating ability of the substituent increases (due to stabilisation of the active centre, increasing the strength of interaction with 1-hexene, which requires a greater activation energy than ethylene) [48].

In a study of the ethylene polymerisation behaviour of a series of $(CpR)_2ZrCl_2$/MAO catalysts (R = H, Me, Et, ^{i}Pr, ^{t}Bu, $SiMe_3$ and CMe_2Ph) [18] a similar ordering of activities, as found for the EAO co-catalysed series discussed above [12], was found, with the exception of the activities for the ^{t}Bu and CMe_2Ph-substituted complexes, which were lower than expected. The low activity of these two catalysts can be explained by intramolecular co-ordination of these substituents to the metal centre, thus inhibiting reaction. This interaction has been described in literature [49]. In the EAO co-catalysed series, this interaction may be prevented by the relatively more bulky EAO co-catalyst molecules.

If the complete set of results is considered, multiple regression versus steric and electronic parameters did not yield statistically significant results, suggesting a more complex, non-linear relationship between the substituent parameters and activity. On a more qualitative basis, the effect seems to be mainly electronic; the most active catalysts have Hammett substituent parameters with $F = 0$. There is a large change in activity over the range of F (−0.02 to 0.05) in this study when compared to values of $F = 0.42$ and 0.45 for Cl and F, respectively. There appears also to be a small steric effect; slightly bulky substituents are needed to protect the metal from bimolecular deactivation, but should not be so bulky as to restrict monomer access. The most active catalysts had θ_1 in the range 143–146°.

If the results for the ^{t}Bu and CMe_2Ph-substituted complexes are excluded, there is a modest negative correlation between polymerisation activity and cga (78% of the variation in the data explained by the regression, $p = 0.03$) (Fig. 10). A similar result is obtained when the cone angle (θ_1) is used in place of the cga (74% of the variation explained, $p = 0.04$) For mono-substituted Cp rings or small substituents, a larger cga leads to lower activity as the ligands provide less protection to the metal centre. Janiak et al. [19,22] has shown that large substituents on Cp rings, or multi-substituted Cp rings, have the inverse trend with respect to cga. Note that here a purely steric effect has been identified; the addition of an electronic term (F) to the regression equation does not yield an improvement in the amount of variation in the data explained by the model.

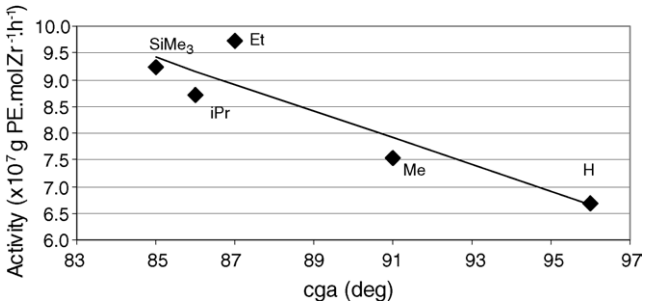

Fig. 10. Correlation between activity data [18] and the cga. The line represents the least-squares fit to the data given by the equation: Activity ($\times 10^7$ g PE mol Zr^{-1} h^{-1}) = −0.25(cga) + 30.75.

The difference between the MAO- and the EAO- co-catalysed series [12] could be related to the bulkier ethyl groups and lower degree of oligomerisation of EAO compared to MAO [32,39c,50–52]. EAO may not interact with the active site as effectively as MAO and thus the steric effects of the catalyst itself become more prominent. Polymerisation conditions were also different. However, it should be noted that, excluding the data for the ^{t}Bu and CMe_2Ph catalysts, the trend in the MAO results is the same as the trend in the EAO results (the linear correlation has an adjusted correlation coefficient (R^2) of 0.81) (Fig. 11) [47].

A study undertaken on a series of $(CpR')(CpR'')TiCl_2/Et_2AlCl{\cdot}Cl_2AlEt$ catalysts (R′ = H, R″ = Me, ^{t}Bu, $SiMe_3$, CMe_2Ph and R′ = R″ = H, Me, Et, ^{i}Pr, ^{t}Bu, $SiMe_3$, CMe_2Ph) [15] showed that polymerisation activity was almost totally dependent on steric factors. The existence of a steric threshold was demonstrated, with only the unsubstituted catalyst and mixed ring catalysts with sterically less demanding substituents having appreciable activity (Fig. 12). No significant correlation between polymerisation activity and linear combinations of steric and electronic parameters (as described above) could be identified, and thus it appears that these catalysts exhibit a 'pure' steric effect in their polymerisation behaviour.

A study of the ethylene polymerisation behaviour of a series of $(1\text{-R-Ind})_2ZrCl_2$ (R = H, Me, Et, ^{i}Pr, ^{t}Bu, $SiMe_3$, Ph, Bz, 1-napthyl) and $(2\text{-R-Ind})_2ZrCl_2$ (R = H, Me, Et, $SiMe_3$, Ph, Bz, 1-napthyl) was undertaken [17]. The substituents were chosen to cover a wide range of steric and electronic

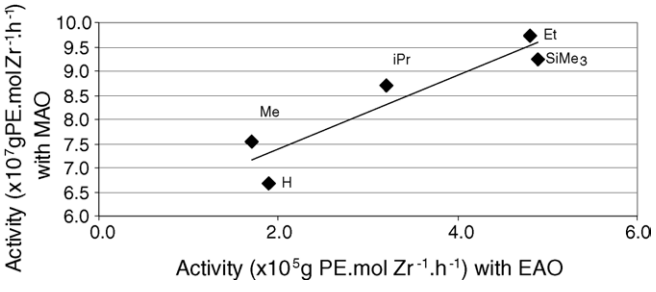

Fig. 11. Correlation between the ethylene polymerisation activities for EAO [12] and MAO [18] catalysed reactions.

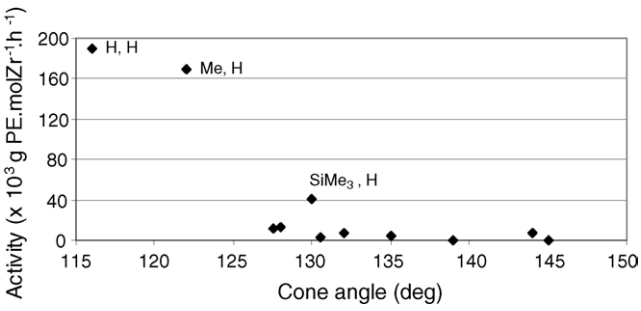

Fig. 12. Plot of ethylene polymerisation activity [15] vs. the average cone angle, θ_1.

properties. Due to the range of polymerisation activities observed, it was necessary to adopt two sets of conditions to obtain a reliable activity series. In the first series, a low concentration of catalyst was used (1.87×10^{-7} M), but this resulted in poor activities for some of the catalysts. In the second series, at a higher catalyst concentration (1.87×10^{-6} M) the activities of these catalysts increased and differentiation of their activities was possible. Simple and multiple regression of the polymerisation activities against steric (cone and solid angle) and electronic (Hammett) parameters yielded no statistically significant models. In general, it was found that substituents equal or larger in size than ^{i}Pr gave poor polymerisation activity. 1-Substituents generally gave higher activities than 2-substituents, the difference being more pronounced the larger the substituent. Rotational barriers during polymerisation may exist. The lower-than-expected activity for the Bz- and ^{t}Bu-substituted complexes could be related to intramolecular co-ordination of the Ph group to the cationic metal centre, thus inhibiting reaction. The 1-$SiMe_3$ complex, although similar in size to the 1-^{t}Bu-substituted complex, has a much higher activity and is thought that the longer C–Si bond places the methyl groups of this substituent further away from metal, thus preventing intramolecular interaction. The 1-napthyl-substituted complex (which has a similar size to the ^{t}Bu complex) has a surprisingly low activity. However, examination of its ligand profile plot shows that the naphthyl group extends further out in space, making the active site less accessible to monomer. The polydispersity (Mw/Mn) of the polymers produced from these catalysts lie in the range 2.0–6.7, indicating multi-site catalysts in some cases. This may have a dramatic effect of the observed activities, thus complicating the correlation of catalyst activity with steric and electronic parameters.

3.2. Measurement of molecular spaces

3.2.1. Methodology

The measurement of molecular spaces was developed by Brintzinger and co-workers as a simple, robust measure for steric accessibility of the metal centre, given that molecular modeling approaches are limited due to the uncertainty with regard to the rotational deformability of ansa-metallocene complexes [20,21].

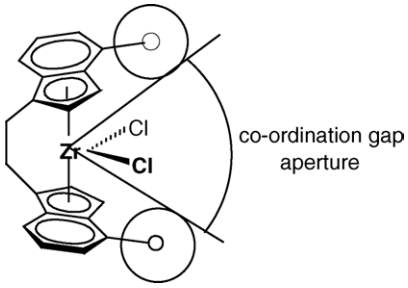

Fig. 13. The co-ordination gap aperture is measured as the largest possible angle between the inner van der Waals surfaces of the β-substituents on the five-membered ring. In this example, a substituted indenyl ring is shown. Figure was reproduced from Ref. [36], with permission of the copyright holders.

The co-ordination gap aperture (cga) measures the amount of space available to a reactant molecule approaching the active metal polymerisation centre. It is defined by the angle formed by two planes, through the metal, which touch the inner van der Waals radii of the β-substituents on the five-membered ring of ansa-metallocene complexes (Fig. 13). These substituents are orientated into a conformation that maximises the cga. The cga differs from the $Cp_{centroid}$–Zr–$Cp_{centroid}$ angle in that it is the largest angle formed by the intersection of the two planes at the metal centre, which touch the inner van der Waals radii of the two Cp groups. Clearly, the size of this angle is intimately linked to the nature of the ligand and its substituents.

A further measure which can be derived from this approach is the co-ordination gap obliquity angle, which is defined by the angle of the 'edge' of the co-ordination gap (i.e. the intersection of the two tangential planes) relative to the plane bisecting the centroid–Zr–centroid angle [20]. In general, there is an inverse relationship between cga and obliquity angle for chiral ansa-metallocenes with one β-substituent and one βH atom at each ring, since obliquity will increase (and cga decrease) with the size ratio of the β-substituents. Chiral ansa-metallocenes which have as β-substituents Me, ^{i}Pr or Cy groups, yield similar cga and obliquity angle values as Ph substituents if one considers these substituents in their least obtrusive conformation. Similarly, β-substituents with a tertiary C atom, such as 1-Me-Cy groups, are practically indistinguishable from ^{t}Bu-substituents in this regard [21].

The cga was originally designed for use with *ansa*-metallocenes where the β-substituents on the C_5 rings influence the size of the gap aperture. The ligands on unbridged metallocenes, however, are usually free to rotate about the $Cp_{centroid}$–Zr axis, making the choice of one specific β-carbon on the C_5 ring less meaningful. By using the cone angles of the Cp ligand (α) and bending angle (β) at the Zr atom, Janiak et al. were able to calculate the cga for a series of substituted $(CpR)_2ZrCl_2$ compounds [19]. For five-fold symmetrically substituted Cp rings, the cga is given by

$$\text{cga} = 360^\circ - \frac{\alpha_1}{2} - \frac{\alpha_2}{2} - \beta \quad (9)$$

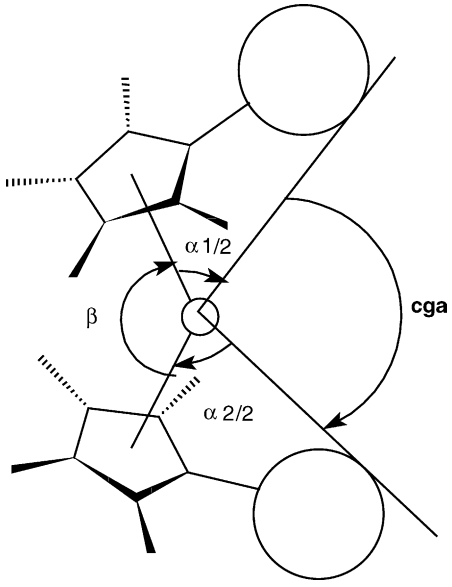

Fig. 14. The co-ordination gap aperture can be calculated from the bending angle, β, of the metallocene and the half cone angle, $\alpha/2$, of its Cp ligands. Figure was reproduced from Ref. [36], with permission of the copyright holders.

where α_1 and α_2 are the cone angles for the two Cp ligands and β the angle between the metal and the two ring centroids (Fig. 14).[2] For mixed ligands of the type $C_5R_{5-n}R'_n$, the cone angle α_i can be approximated by

$$\alpha_i = \frac{5-n}{5}\alpha + \frac{n}{5}\alpha' \quad (10)$$

where α and α' are the cone angles of the corresponding five-fold symmetrically substituted ligands.[3] These calculations are based on the assumption of unhindered ring rotation; this may not be true once the Cl atoms in $(CpR)_2ZrCl_2$ are replaced by bulkier entities, such as growing polymer chains [39b,d,e,g,i].

The lateral extension angle measures the angle formed between two planes, also through the metal, but which touch the van der Waals radii of the two α-substituents on either side of the complex (Fig. 15) [20,21].

In recent years the so called 'ansa' effect has been elicited to describe the special effect that is associated with the size of the ansa backbone in metallocene catalysts and how this effect could impact on the electronic and steric effects and resultant catalytic activity associated with the metal center [53]. A geometrical analysis of a range of complexes (non-bridged and ansa) of the type Cp_2MX_2 has also been conducted in terms of geometrical measures and electronic factors [54].

[2] For example, the cga for $(C_5Me_5)(C_5H_5)ZrCl_2$ is calculated as follows: $\alpha_1 = 171^\circ$ (for C_5Me_5), $\alpha_2 = 139^\circ$ (for C_5H_5), $\beta = 130^\circ$ and thus the cga = 75° (see Table 1 for more data).

[3] For example, the cga for $(C_5Me_4H)(C_5H_5)ZrCl_2$ is calculated as follows: $\alpha_1 = 164^\circ$ (for C_5Me_4, calculated from $\alpha = 139^\circ$ (for C_5H_5), $\alpha' = 171^\circ$ (for C_5Me_5), $n = 4$ and thus $\alpha_1 = 164^\circ$), $\alpha_2 = 139^\circ$ (for C_5H_5), $\beta = 132^\circ$ and thus the cga = 76° (see Table 1 for more data).

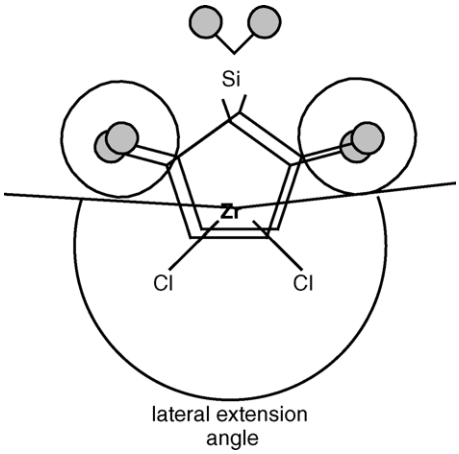

Fig. 15. The lateral extension angle is the angle formed between the two vectors, originating at the metal, which touch the van der Waals outline of the two α-substituents on either side of the complex. Figure was reproduced from Ref. [36], with permission of the copyright holders.

In the geometric methodology, a procedure similar to that used by Brintzinger and Janiak was used (see above). However, the main emphasis in this study was how the size of the ansa backbone influenced the geometry of the resulting complexes. The data clearly revealed that the bridge size had a major impact on the space available at the metal for reaction with incoming reactants. The geometrical measures used and the results obtained are shown in Fig. 16 and Table 4 [54a].

3.2.2. Applications

The concepts of co-ordination gap aperture and lateral extension angle were used to rationalise the propylene polymerisation behaviour of a number of chiral ansa-metallocene/MAO catalysts [55]. Complexes with a trimethylene link between the Si bridge atom and an α-position of each C_5 ring ligand (and with ^{i}Pr and ^{t}Bu groups as β-substituents) were compared to their Me_2Si-bridged analogs. The ^{t}Bu-substituted spirosilane complex yielded a polymer with a relatively high content of 3,1-insertions, which appeared to be associated with decreased co-ordination gap aperture and increased lateral extension angles of the spirosilane-bridged zirconocene complexes, which favour 2,1-insertions and consequently, the incorporation of 3,1-units into the polymer.

In a study of the ethylene polymerisation activity of a series of mixed-ring zirconocene complexes (CpR)(CpR′)$ZrCl_2$/MAO (CpR = CpR′ = C_5H_5, C_5Me_4H, C_4Me_4P, C_5Me_5, ^{t}BuC_5H_4, 1,3-^{t}Bu$_2C_5H_3$, and CpR = C_5H_5, CpR′ = C_5Me_4H, C_4Me_4P, C_5Me_5, ^{t}BuC_5H_4, 1,3-^{t}Bu$_2C_5H_3$, 1,2,4-^{t}Bu$_3C_5H_2$) [19,22], Janiak et al. found that for each series (Me and ^{t}Bu) relative activity could be ordered on steric grounds, with the unsubstituted zirconocene more active than the mixed sandwiches and these, in turn, more active that the symmetrically substituted zirconocenes.

Reactions were carried out at different catalyst concentrations and Al:Zr ratios to elucidate the role of polymerisation conditions on the relative activity of the complexes. It was found that at a zirconium concentration of 2.5×10^{-7} M together with an Al:Zr ratio of 160,000:1 the reaction rate lies below or around the diffusion rate limit, so that the activity profiles show a constant ethylene consumption. The lower amount of polyethylene produced in these experiments assured the existence of a homogeneous phase over an extended time period (the highly active Cp_2ZrCl_2 system being a notable exception). Consequently, other things being equal, the difference in activities should reflect the searched for difference in steric or electronic characteristics [22].

The activities of the methyl-substituted Cp complexes showed a good linear dependency on cga (adjusted $R^2 = 0.988$, $p = 0.0003$). Regression of activity data for these complexes against solid angle (Ref. [41], mixed ring angles were interpolated) and cone angle values gives as good a model (Fig. 17).

The activities of the ^{t}Bu-substituted Cp complexes indicated that a minimum cga of about 50° is needed for any appreciable activity at all under these conditions, indicating the presence of a steric threshold (Fig. 18). Compared to the data for the methyl series, the cga for the ^{t}Bu-substituted complexes may be too large if a purely steric effect is assumed (since the activities are lower than the methyl series for same cga). The possibility of rotamers with the ^{t}Bu groups pointing along the maximum opening where the polymerisation reaction takes place is not ruled out, so that the actual cga

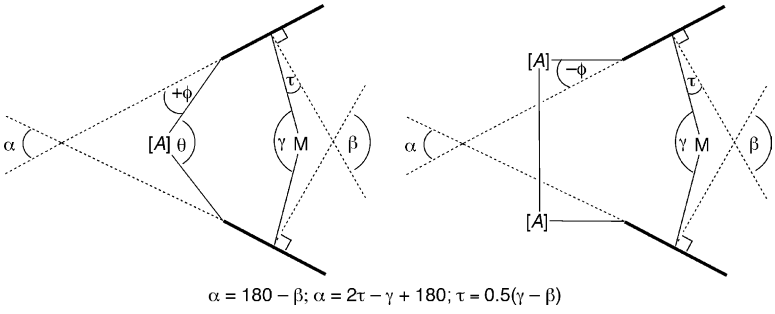

Fig. 16. Parameters to define metallocene geometries, as illustrated for single- and double-atom bridges. α = Interplanar ring angle; $\beta = Cp_{norm} - Cp_{norm}$ angle ($\alpha + \beta = 180°$); $\gamma = Cp_{centroid}$–M–$Cp_{centroid}$ angle; $\tau = 0.5(\gamma - \beta)$ = tilt angle (the angle between the M–$Cp_{centroid}$ vector and the ring normal); $\theta = C_{ipso}$–A–C_{ipso} angle, where A represents a bridging atom; $\phi = 180° - (A - C_{ipso} - Cp_{centroid})$, the angle between the A – C_{ipso} vector and the Cp mean plane. Figure was reproduced from ref. [54], with permission of the copyright holders.

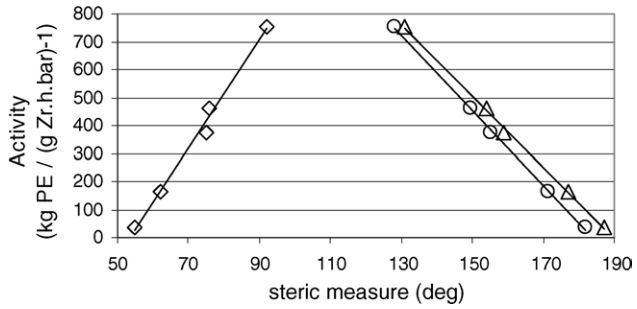

Fig. 17. Plots of ethylene polymerisation activity [19,22] (for Me-substituted complexes) vs. steric measures: ◊, cga; ◯, cone angle; △, solid angle. Data were taken from the original references and replotted.

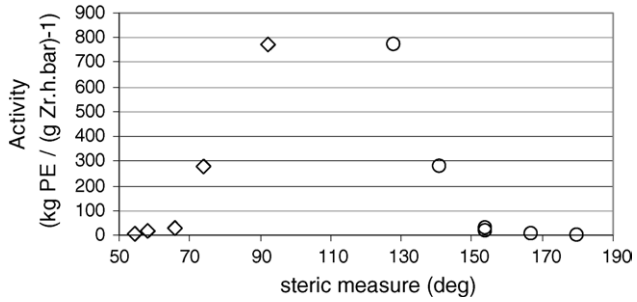

Fig. 18. Plots of ethylene polymerisation activity [19] (for ^{t}Bu-substituted complexes, lower Zr concentration) vs. steric measures: ◊, cga; ◯, cone angle. Data were taken from the original reference and replotted.

may be smaller than estimated, effectively blocking reaction, thus lowering the number of active species.

Interestingly, the activities of the ^{t}Bu-substituted Cp complexes at a higher Zr concentration (for which some of the Me-substituted complexes demonstrated diffusion-controlled behaviour), which results in all the complexes having appreciable activity (no steric threshold), are linearly related to cga (adjusted $R^2 = 0.82$, $p = 0.0008$) (Fig. 19).

The lowest activities were found for the phospholyl complexes, probably due to adduct formation between aluminium species from MAO and the phosphorus donors, thereby changing the steric features of the catalytic centre [19].

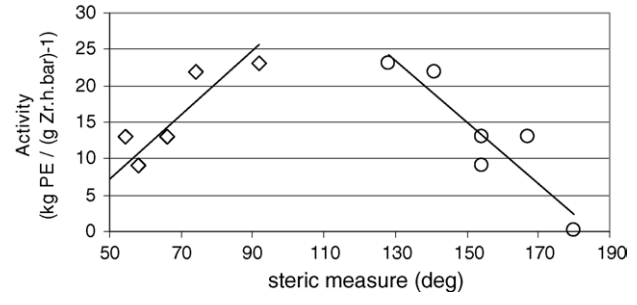

Fig. 19. Plots of ethylene polymerisation activity [19] (for ^{t}Bu-substituted complexes, higher Zr concentration) vs. steric measures: ◊, cga; ◯, cone angle. Data were taken from the original reference and replotted.

3.3. Taft steric parameter

3.3.1. Methodology

Taft defined the steric parameter, E_S as

$$E_S = \log\left(\frac{k}{k_0}\right) \quad (11)$$

where the rate constant, k_0, refers to the reference Me-substituted ester and k the rate constant for the acid-catalysed hydrolysis of a substituted ester [56]. Although Taft's steric parameter was averaged from four measurements, it was clear that the parameter contained resonance effects. Attempts to modify the defining equation to exclude these effects have been made. Hancock et al. [57] proposed

$$E_S = E_S^0 + (-0.306)(n - 3) \quad (12)$$

where n is the number of α-H atoms in the substituent. Pal'm [58] defined

$$E_S = E_S^0 - 0.33(n_H - 3) - 0.13(n_C) \quad (13)$$

where n_H is the number of α-H and n_C the number of α-C atoms in the substituent.

Charton determined that the Taft steric parameter was free of electronic effects [59] and that E_S^0 was an electronic parameter depending on σ_1 and σ_R (localised and delocalised substituent constants, respectively) [60].

3.3.2. Applications

Bravaya and co-workers have conducted a number of studies [23,61–63] in which specific catalyst activity $(A_R - A_H)/A_H$ (where A_R and A_H are the activities of the R-substituted and unsubstituted complex, respectively) could be correlated with a linear combination of the Taft electronic parameter, σ^* [45], and the Pal'm steric parameter, E_S^0 [58]. (A good correlation of these parameters with electrochemical reduction potentials of zirconocene complexes has been established [64].) Simple regressions of polymerisation activity against both of these parameters in turn were statistically not significant, indicating that a combination of steric and electronic effects was required to explain catalyst activity. (Note that similar results are obtained with regressions using the actual activity of each catalyst rather than the specific activity.) To be noted is the low ethylene pressures (0.54–1.0 atm) used in these studies. It is argued that, at ethylene pressures at or below 1 atm, diffusion from the gas into the liquid phase becomes the rate-limiting step. The differences in activity then represent differences in activation equilibria and thus a difference in the active species concentration [22].

The effect of substituents on the ethylene polymerisation activity of 2-substituted indenyl zirconium catalysts, (2-R-Ind)$_2$ZrCl$_2$/MAO (R = Ph, *p*-Tol, Me, ^{i}Pr, Cy and 1-allyl) was studied [61]. Regression of the relative activities for these complexes against the Taft electronic and the Taft steric parameter (E_S^0, different values to the Pal'm parameter used in the other three studies by the same authors) provided an ex-

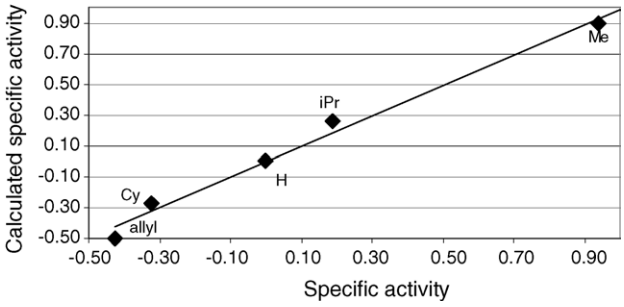

Fig. 20. Plot of calculated vs. actual activity data [61]. The line represents the least-squares fit to the data given by the equation: Specific activity = $-2.48(E_S^0) + 1.29(\sigma^*)$. Data were taken from the original reference and replotted.

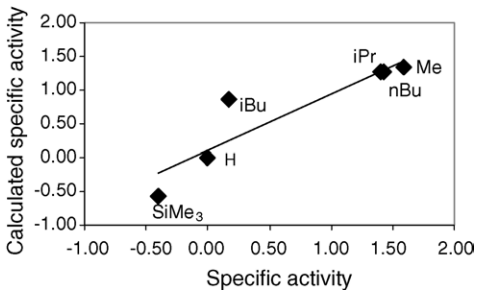

Fig. 22. Plot of calculated vs. actual activity data [63]. The line represents the least-squares fit to the data given by the equation: $\ln(R^0_{CpR}/R^0_{CpH}) = -3.13(E_S^0) + 0.79(\sigma^*)$. Data were taken from the original reference and replotted.

cellent correlation (97% of the variance accounted for by the model; $p = 0.01$) (Fig. 20). The authors noted that the electronic effect dominates by comparing the coefficients of the steric and electronic parameters in the regression equation. These parameters should, however, be scaled by multiplying them by the range of the steric and electronic parameters, thus modifying the result and giving a 56% contribution by steric effects and a 44% contribution by electronic effects. Catalyst activity decreases as the electron-donating ability of the substituents increases and as their size increases. (The authors' interpretation is that the electronic effect dominates not only through the electron-donating/withdrawing ability of the substituents, but also by increasing the lability of the indenyl system towards ring slippage effects, thus lowering the steric effect.)

A study of the effect of substituents on the ethylene polymerisation activity of substituted Cp zirconium catalysts, $(RCp)_2ZrCl_2$/MAO (R = H, Me, ^{i}Pr, ^{i}Pr$_2$, ^{n}Bu, ^{i}Bu, ^{t}Bu, Me$_5$, SiMe$_3$, Cy and Cy$_2$) was carried out by the same authors [23]. Regression of the relative activities for these complexes against the Taft and Hammett parameters indicated that two sub-series of catalysts existed (Fig. 21). The series including R = H, Cy, Cy$_2$ and SiMe$_3$ showed increased activity with increased substituent size and increased electron-donating ability of the substituent. The second series (comprising the remaining catalysts, all alkyl-substituted) showed increased activity with decreasing size and decreasing electron-donating ability. The latter group of alkyl-substituted catalysts has turnover numbers, which vary strongly with steric and electronic parameters, while the turnover number of the first group are essentially invariant with respect to these parameters. This suggests that the alkyl substituents participate in reactions responsible for chain termination and regeneration of the active centre. In a closely related study (R = H, Me, ^{i}Pr, ^{n}Bu, ^{i}Bu and SiMe$_3$; co-catalyst Al^{i}Bu$_3$/CPh$_3$B(C$_6$F$_5$)$_4$) [62,63], the authors found a similar dependence of the logarithm of the ratio of the initial ethylene consumption rate (R^0) for the substituted and unsubstituted catalysts, $\ln(R^0_{CpR}/R^0_{CpH})$, with the Taft and Hammett parameters (Fig. 22). (The ratio of initial rates was used as the kinetics of the catalysts differed substantially under these experimental conditions.) With this co-catalyst system, the catalysts are more sensitive to the electronic effect of the substituents than with MAO as co-catalyst.

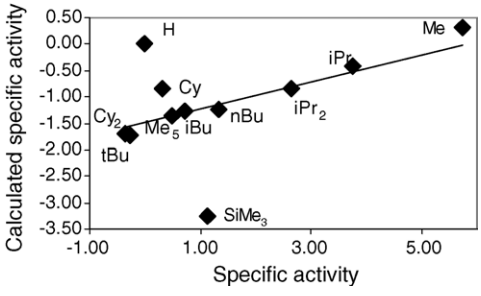

Fig. 21. Plot of calculated vs. actual activity data [23]. The line represents the least-squares fit to the data given by the equation: Specific activity = $-1.20(E_S^0) + 1.12(\sigma^*) + 2.53$. Data were taken from the original reference and replotted.

3.4. Theoretical approaches

An alternative procedure that bypasses the conventional methods described above is to use a theoretical approach to the evaluation of parameters that affect catalyst activity. Some of these approaches which have been applied to zirconocene-type catalyst systems are listed below.

The influence of the ligand structure of 54 bridged zirconocene polymerisation catalysts on the accessibility of the active reaction centre was studied by an ab initio Hartree-Fock method [65]. Although the treatment of transition metal complexes by ab initio molecular orbital methods is generally difficult, due to near-degeneracy and relativistic effects, these effects are small for zirconium and so it was found that the HF/3-21G* method produced reasonably accurate geometries for zirconocenes (by comparison to crystal structure data) and was capable of reproducing the expected trends in the changes of the geometry parameters for the series of catalysts. Both geometrical and stability parameters were calculated and optimised.

The steric influence of the ligand framework can be understood in terms of the following factors which increase the accessibility of the active site: increasing Zr–Cp$_{centroid}$ dis-

tance, increasing $Cp_{centroid}$–$Cp_{centroid}$ plane angle, decreasing $Cp_{centroid}$–Zr–$Cp_{centroid}$ angle and decreasing orientation of ligand substituents towards the active site. The electron-donating influence of the ligand framework is related to the following factors (steric factors being equal): increasing Zr–$Cp_{centroid}$ distance, increasing ring slippage angle and increasing $Cp_{centroid}$–Zr–$Cp_{centroid}$ which provides more shielding for the metal.

Comparisons to experimental data were limited to qualitative trends, due to dissimilar reaction conditions in various sources. General conclusions determined are noted below: (i) Modifications on the *bridging* unit have both steric and electronic influences. Short bridges provide decreased steric hindrance of the ligand framework, but also reduced shielding for the cationic metal resulting in decreased stability of the cation. The influence of long bridges is opposite, with lowered steric hindrance, but increased shielding and stability of the cation. (ii) Modifications on the *substituted Cp ligand* have mostly electronic consequences. Increased aromaticity of the ligand improves its capability of donating electrons to the electron-deficient metal, which stabilizes the cation. The increase in relative stability of the cation as a function of the number of aromatic carbons is systematic. The improved accessibility of the cationic metal due to the increased relative stability of the cation shows correlations with experimental activity data. Electron-withdrawing substituents attached to the Cp ligand destabilise the cation due to the decreased electron-donating capability of the Cp ligand. The resulting reduced concentration of active catalyst centers can be seen in decreased polymerization activities. The opposite influence of electron-donating substituents is equally evident. However, increased stability of the cation, obtained by increased electron-donating capability of the Cp ligand, does not inevitably provide highly active catalysts. (iii) The electronic nature of the ligand is further influenced by *coordination of the hard Lewis acidic co-catalyst* to the hard Lewis basic ligand substituents, leading to inductive electron withdrawal which converts electron-donating substituents to electron-withdrawing ones, resulting in decreased polymerisation activity. This unfavorable coordination of the co-catalyst to hard Lewis basic substituents can be complicated by introducing steric bulk around the donor atom.

An investigation into the catalytic activity of a series of unbridged, alkyl-substituted metallocenes, $(CpR)_2ZrCl_2$ (R = H, Me, 1,2-Me_2, 1,3-Me_2, 1-Me-2-Et, ^{n}Pr, ^{n}Bu, Me_4, Me_5) was undertaken by Rytter and co-workers [66]. Using quantitative structure-activity relationship (QSAR) modeling, the propagation rate constant, derived from kinetic modeling of the activity-time profile, was related to changes in 17 geometric and electronic descriptors derived from quantum-chemical (QM) calculations on a transition state model for each catalyst. After exclusion of the 1-Me-2-Et catalyst as an outlier, the final model, using one principal component, indicated that the propagation rate constant was positively correlated with descriptors related to the size of the catalyst (principal moment of inertia, radius of gyration, and the number of rotatable bonds), as well as with the partial charge on Zr and increasing Cp–Cp angle. Negative correlations were found with the LUMO–HOMO energy gap and the Zr–H_γ distance ($r^2 = 0.75$ after leave-one-out cross-validation). Models constructed using the catalytic activity over one hour of reaction time were significantly worse than those based on the propagation rate constant, probably owing to the different kinetic profiles of the different catalysts.

Rytter and co-workers also investigated the ethylene homopolymerisation and ethylene/1-hexene copolymerisation behaviour for all methyl-substituted $(R_nC_5H_{5-n})_2ZrCl_2$/MAO catalytic systems (R = H, Me, 1,2-Me_2, 1,3-Me_2, 1,2,3-Me_3, 1,2,4-Me_3, Me_4, Me_5) [67,68]. Generally, an increasing number of methyl substituents on the Cp ligand resulted in lower 1-hexene incorporation in the polymer; however, the two catalysts with split methyl substitution (R = 1,3-Me_2, 1,2,4-Me_3) showed a higher co-monomer response than their di- and tri-substituted counterparts (R = 1,2-Me_2, 1,2,3-Me_3). In order to rationalise this behaviour, quantum mechanical (QM) calculations based on density functional theory (DFT) were used to model a Cossee-like transition state and mechanism of chain propagation, both with ethylene and 1-butene (to model a longer α-olefin). Linear relationships between the measured copolymer melting temperatures (T_m) and structural parameters derived from the QM calculations were analysed by a partial least-squares (PLS) algorithm. The following parameters were used: (i) ΔE(TS), the energy difference (in the transition state) of 1-butene and ethylene insertion, (ii) S_Φ, the sum of two dihedral angles believed to measure the steric repulsion of α-olefin insertion, (iii) S_r, the sum of two distances from C3 of 1-butene and C_γ of the growing polymer chain, to the central plane defined by Zr, C1 and C_α, (iv) V_{HH}, the total overlapping volume of 1-butene insertion between van der Waals spheres centered in H atoms and (v) $\theta(\gamma)$, the opening angle between the two (average) planes defined by the C atoms of the Cp rings, measured in the γ-agostic configuration of the catalyst [67].

The resulting model, based on two principal components, yielded r^2 values of 0.87 for the calibration and 0.78 after leave-one-out cross-validation. The regression coefficients revealed positive correlations between T_m and ΔE(TS), S_Φ and V_{HH} and negative correlations with S_r and $\theta(\gamma)$ as expected. The results indicated that a small Cp–Cp opening angle correlates with high T_m values mainly due to the presence of the R = Me_5 catalyst in the data set. However, weak steric hindrance (i.e. large S_r and small S_Φ) in the transition state resulted in relatively low values of T_m (i.e. high levels of co-monomer incorporation) for R = H, the opposite being true for R = Me_4.

Comparable polymerisation data were then obtained for three tetramethyldisilylene-bridged zirconocene catalysts [67]. The model derived above was almost able to predict the observed co-monomer responses for these three catalysts, but did predict the correct trend. Inclusion of the data for these three catalysts with the eight catalysts analysed above, gave rise to a model with a single principal compo-

nent based on the parameters $\theta(\gamma)$, V_{HH}, and either S_r or S_Φ ($r^2 = 0.78$ for calibration and 0.66 after leave-one-out cross-validation). Linear regression models of the same quality as for the copolymer T_m could not be constructed for the mol% 1-hexene incorporated into the polymer.

The concept of paired interacting orbitals (PIO) has recently been applied to polymerisation catalysts [69,70]. In brief, the method determines which molecular orbitals play a dominant role in the chemical reaction between two systems. Interactions are represented in terms of a few pairs of localised orbitals. In each pair, one orbital belongs to the catalyst and one to the reactant (alkene). As the reactant approaches the catalyst, deformation of the structure begins to take place along with electron delocalisation from existing bonds to the reaction regions. This electron delocalisation is the driving force of the reaction Since the reaction regions and the amount of delocalised electrons are determined by the PIO and the overlap population of the PIO, the larger the amount of the total overlap population of all PIO's (ΣPIO), the more easily the reaction proceeds. Thus ΣPIO may be used as a predictor of relative polymerisation activity and regio- and stereo-selectivity.

Propylene insertion and chain transfer were studied for a series of $[^{i}BuZrH_2SiL_2]^{+1}$ complexes (L = Cp, 2-MeCp, 3-MeCp, 4-MeCp, 5-MeCp, Ind, 2-MeInd, 3-MeInd) [70] using molecular orbitals based on the extended Hückel method and the PIO approach described above. Calculations were carried out with the *LUMMOX*™ system [71]. The relative rates of insertion and chain transfer to monomer, and thus the relative molecular weights of the polymers, for the series of catalysts was estimated and found to be in good agreement with the experimental results presented by Spaleck et al. [72].

Recently, a first attempt at using three-dimensional quantitative structure–activity relationship (3D-QSAR) methodology to predict the ethylene polymerisation behaviour of metallocene catalysts was reported [73]. The underlying concept of 3D-QSAR (used extensively in drug design) is that differences in a target property (in this case, polymerisation activity and polymer molecular weight) are related to differences in the shapes and intensities of the molecular fields describing the tested molecules [74]. 3D-QSAR methods identify spatial regions of a given molecule (the monomer) which match the binding site of the receptor (catalyst).

The study comprised seven structurally diverse metallocene catalysts, co-catalysed by MAO. The statistical robustness of the derived 3D-QSAR model suggests that further work should be carried out with more catalysts. Variation in polymerisation activity data could be successfully explained in terms of steric and electronic fields. The model predicts that an increase in the Cp–Zr–Cp angle and/or incorporation of bulky ligands will increase catalyst activity. The electronic interaction is related to the LUMO molecular orbital and local softness parameters. The arrangement of aromatic ligands around the metal centre as well as the chemical nature of the ligand (Cp or Ind) contributed to explaining the variance in the experimental data. Polymer molecular weight was found to correlate well with the LUMO and local softness fields; the Cp–Zr–Cp angle is the key geometric variable enabling a particular distribution in the LUMO and local softness fields that lead to increased molecular weight. The steric field did not contribute significantly to the model for molecular weight. These results indicate that the 3D-QSAR method may serve to identify the main structural features required to develop better metallocene catalysts for olefin polymerisation.

Some years ago Brown and co-workers developed a method to quantify steric effects of ligands using repulsive repulsive energies, E_R, a method that uses a linear free energy approach [76]. The MMP2 programme (molecular mechanics) was used to evaluate the ligand energies. As was noted cone and solid angles correlated well with E_R values. This methodology could thus provide another alternative to evaluating the steric effect in substituted Cp ligands.

4. Conclusions

It will be seen from the above review that many attempts have been made to both separate out steric effects (from electronic effects) and to give some quantitative measure to a steric effect. The problem relates to generating a reliable, general procedure that can provide a value (preferably easily measured) for any ligand. In general ground state structures are used for the steric calculations. Remarkably, most steric measures generate similar values for ligands [10] while a knowledge of the assumptions used in any measure allows one to appreciate the limitations and differences associated with a specific steric 'number'. Remarkably all measures give similar 'numbers' suggesting that while fine tuning allows for corrections to be made, the intuitive sense of ligand size generated to date is correct.

The issue then relates to the ability of the steric number to be associated with a reactivity parameter, in this instance a polymerisation rate. All the data generated to date indicate the presence of a steric threshold in metallocene catalysts and once this threshold is exceeded both electronic and steric factors will come into play and impact on catalyst activity. The data generated by a range of authors all show similar trends – a variable degree of electronic/steric control on activity – again suggesting that the general philosophy is correct. However, the procedures still appear too crude to allow for new catalyst development.

An alternative approach is to evaluate the size of the reaction site. This is in keeping with the concept of a reaction cavity at the metal centre, a site that will be constrained in size by the surrounding ligand set. Can this cavity be adequately represented and, if so, will the cavity size/shape provide an ability to predict reaction rates? The cga approach has had limited success in this respect. A reaction cavity concept has however been developed in the context of reactions in the solid state (Ohashi) and it is possible that this approach may allow a more predictable model of metallocene polymerisation catalysts. However, a key difficulty with this approach

relates not only to the ability to accurately measure a cavity BUT also to establish which ground or transition state structure should be used to generate the cavity.

Acknowledgements

We wish to thank the University of the Witwatersrand, AECI Limited, the National Research Foundation (NRF) and the Technology and Human Resources for Industry Programme (THRIP) for financial support that allowed the original work to be initiated. Mr. Alan Cameron (SASOL Polymers) and Mr. Frank Fisher, AECI Limited, are also thanked for their support over the years. Finally, thanks to the many students who carried out the various studies and also to Dr. John Mellor and Dr. Neil Grimmer (both of SASOL) for assistance with the literature and figure collection.

References

[1] (a) G. Wilkinson, F.G.A. Stone, E.W. Abel (Eds.), Comprehensive Organometallic Chemistry, Pergamon, New York, 1982;
(b) E.W. Abel, F.G.A. Stone, G. Wilkinson (Eds.), Comprehensive Organometallic Chemistry II, Pergamon, New York, 1995.
[2] (a) H.H. Brintzinger, D. Fischer, R. Mülhaupt, B. Rieger, R.M. Waymouth, Angew. Chem. Int. Ed. Engl. 34 (1995) 1143;
(b) J.A. Gladysz (Ed.), Chem Rev. 100 (2000) 1167.
[3] W.P. Long, D.S. Breslow, J. Am. Chem. Soc. 82 (1960) 1953.
[4] W. Kaminsky, K. Külper, S. Niedoba, Makromol. Chem., Macromol. Symp. 3 (1986) 377.
[5] W. Kaminsky, K. Külper, H.H. Brintzinger, F.R.W.P. Wild, Angew. Chem. Int. Ed. Engl. 24 (1985) 507.
[6] (a) J.A. Ewen, Stud. Surf. Sci. Catal. 25 (1986) 271;
(b) J.A. Ewen, J. Am. Chem. Soc. 106 (1984) 6355;
(c) J.A. Ewen, Sci. Am. 276 (1997) 86.
[7] P. Corradini, G. Guerra, L. Cavallo, Acc. Chem. Res. 37 (2004) 231.
[8] M.O. Albers, N.J. Coville, Coord. Chem. Rev. 53 (1984) 227.
[9] (a) P. Johnston, M. Loonat, W.L. Ingham, L. Carlton, N.J. Coville, Organometallics 6 (1987) 2121;
(b) K. du Plooy, C.F. Marais, L. Carlton, R. Hunter, J.C.A. Boeyens, N.J. Coville, Inorg. Chem. 28 (1989) 3855;
(c) N.J. Coville, M.S. Loonat, D. White, L. Carlton, Organometallics 11 (1992) 1082.
[10] D. White, N.J. Coville, Adv. Organomet. Chem. 36 (1994) 95.
[11] P.C. Möhring, N.J. Coville, J. Organomet. Chem. 479 (1994) 1;
See also G.F. Swiegers, Chemtracts 10 (1997) 925.
[12] P.C. Möhring, N.J. Coville, J. Mol. Catal. 77 (1992) 41.
[13] C.A. Tolman, J. Am. Chem. Soc. 92 (1970) 2953.
[14] C.A. Tolman, Chem. Rev. 77 (1977) 313.
[15] P.C. Möhring, N. Vlachakis, N.E. Grimmer, N.J. Coville, J. Organomet. Chem. 483 (1994) 159.
[16] P.C. Möhring, N.J. Coville, J. Mol. Catal. A: Chem. 96 (1995) 181.
[17] N.E. Grimmer, N.J. Coville, C.B. de Koning, J. Organomet. Chem. 642 (2002) 195.
[18] N.E. Grimmer, N.J. Coville, C.B. de Koning, J. Mol. Catal. A: Chem. 188 (2002) 105.
[19] C. Janiak, K.C.H. Lange, U. Versteeg, D. Lentz, P.H.M. Budzelaar, Chem. Ber. 129 (1996) 1517.
[20] K. Hortmann, H-H. Brintzinger, New J. Chem. 16 (1992) 51.
[21] P. Burger, K. Hortmann, H-H. Brintzinger, Makromol. Chem., Macromol. Symp. 66 (1993) 127.
[22] C. Janiak, U. Versteeg, K.C.H. Lange, R. Weimann, E. Hahn, J. Organomet. Chem. 501 (1995) 219.
[23] N.M. Bravaya, V.V. Strelets, Z.M. Dzhabieva, O.N. Babkina, V.P. Maryin, Russ. Chem. Bull. 47 (1998) 1491.
[24] (a) G. Fink, W. Zoller, Makromol. Chem. 182 (1981) 3265;
(b) G. Fink, W. Fenzyl, R. Mynott, Z. Naturforsch 40b (1985) 158.
[25] W. Kaminsky, R. Engehausen, K. Zoumis, W. Spaleck, J. Rohrmann, Makromol. Chem. 193 (1992) 1643.
[26] (a) T. Uozumi, K. Soga, Makromol. Chem. 193 (1992) 823;
(b) C. Janiak, K.C.H. Lange, P. Marquardt, Macromol. Rapid Commun. 16 (1995).
[27] M.P. Thornberry, N.T. Reynolds, P.A. Deck, F.R. Fronczek, A.L. Rheingold, L.M. Liable-Sands, Organometallics 23 (2004) 1333.
[28] K.H. Reichert, K.R. Meyer, Makromol. Chem. 169 (1973) 163.
[29] B. Rieger, C. Janiak, Angew. Makromol. Chem. 215 (1994) 35.
[30] W. Kaminsky, K. Külper, S. Niedoba, Makromol. Chem., Makromol. Symp. 3 (1986) 377.
[31] J.C.W. Chien, B.-P. Wang, J. Polym. Sci. A: Polym. Chem. 26 (1988) 3089.
[32] W. Kaminsky, M. Miri, H. Sinn, R. Woldt, Makromol. Chem., Rapid Commun. 4 (1983) 417.
[33] C. Janiak, B. Rieger, R. Voelkel, H.G. Braun, J. Polym. Sci. A: Polym. Chem. 31 (1993) 2959.
[34] K.A. Bunten, L. Chen, A.L. Fernandez, A.J. Poë, Coord. Chem. Rev. 233–234 (2002) 41.
[35] (a) A.L. Fernandez, C. Reyes, A. Prock, W.P. Giering, J. Chem. Soc., Perkin Trans. 2 (2000) 1033;
(b) A.L. Fernandez, M.W. Wilson, A. Prock, W.P. Giering, Organometallics 20 (2001) 3429;
(c) D. Woska, A. Prock, W.P. Giering, Organometallics 19 (2000) 4629.
[36] N.E. Grimmer, N.J. Coville, S. Afr. J. Chem. 54 (2001) 118.
[37] P.M. Maitlis, Chem. Soc. Rev. (1981) 1.
[38] N.J. Coville, M.S. Loonat, D. White, L. Carlton, Organometallics 11 (1992) 1082.
[39] (a) D.T. Mallin, M.D. Rausch, E.A. Mintz, A.L. Rheingold, J. Organomet. Chem. 381 (1990) 35;
(b) G. Erker, Pure Appl. Chem. 61 (1989) 1715;
(c) R.A. Howie, G.P. McQuillan, D.W. Thompson, G.A. Lock, J. Organomet. Chem. 303 (1986) 213;
(d) R. Been, H. Grondey, R. Nolte, G. Erker, Organometallics 7 (1988) 777;
(e) G. Erker, T. Mühlenbernd, J. Organomet. Chem. 319 (1987) 201;
(f) C. Krüger, M. Nolte, G. Erker, S. Thiele, Z. Naturforsch. 47b (1992) 995;
(g) G. Erker, T. Mühlenbernd, R. Been, A. Rufinska, Y.-H. Tsay, C. Krüger, Angew. Chem., Int. Ed. Engl. 24 (1985) 321;
(h) G. Erker, R. Nolte, C. Krüger, R. Schlund, R. Been, H. Grondey, R. Mynott, J. Organomet. Chem. 364 (1989) 119;
(i) G. Erker, R. Nolte, G. Tainturier, A. Rheingold, Organometallics 8 (1989) 454;
(j) G. Erker, T. Mühlenbernd, A. Rufinska, R. Been, Chem. Ber. 120 (1987) 507;
(k) G. Erker, Pure Appl. Chem. 63 (1991) 797.
[40] A. Immirzi, A. Musco, Inorg. Chim. Acta 25 (1977) L41.
[41] D. White, B.C. Taverner, P.G.L. Leach, N.J. Coville, J. Comput. Chem. 14 (1993) 1042.
[42] B.C. Taverner, Steric, 1.12B (this program may be downloaded via the internet from the following URL: http://www.gh.wits.ac.za).
[43] S.J. Mackie, M.C. Baird, Organometallics 11 (1992) 3712.
[44] (a) D. White, B.C. Taverner, P.G.L. Leach, N.J. Coville, J. Organomet. Chem. 478 (1994) 205;
(b) B.C. Taverner, J.M. Smith, D.P. White, N.J. Coville, S. Afr. J. Chem. 50 (1997) 59;
(c) J.M. Smith, B.C. Taverner, N.J. Coville, J. Organomet. Chem. 530 (1997) 131.
[45] C. Hansch, A. Leo, R.W. Taft, Chem. Rev. 91 (1991) 165.

[46] L. Siergiejczyk, L. Synoradzki, J. Organomet. Chem. 311 (1986) 253.
[47] The data were re-analysed by the authors in preparation of this publication.
[48] C. Pellecchia, A. Proto, P. Longo, Z. Zambelli, Makromol. Chem., Rapid Commun. 12 (1991) 663.
[49] (a) X. Yang, C.L. Church, T.J. Marks, J. Am. Chem. Soc. 116 (1994) 10015;
(b) L. Jia, X. Yang, C.L. Stern, T.J. Marks, Organometallics 16 (1997) 842;
(c) L.H. Doerrer, M.L.H. Green, D. Häussinger, J. Sassmannshausen, J. Chem. Soc., Dalton Trans. (1999) 2111.
[50] W. Kaminsky, R. Steiger, Polyhedron 7 (1988) 2375.
[51] D.J. Cardin, M.F. Lappert, C.L. Raston, Chemistry of Organo-zirconium and -Hafnium Compounds, Wiley, New York, 1986.
[52] E. Giannetti, G.M. Nicoletti, R. Mazzocchi, J. Polym. Sci., Polym. Chem. Ed. 23 (1985) 2117.
[53] H. Lee, P.J. Desrosiers, I. Guzei, A.L. Rheingold, G. Parkin, J. Am. Chem. Soc. 120 (1998) 3255.
[54] (a) C.E. Zachmanoglou, A. Docrat, B.M. Bridgewater, G. Parkin, C.G. Brandow, J.E. Bercaw, C.N. Jardine, M. Lyall, J.C. Green, J.B. Keister, J. Am. Chem. Soc. 124 (2002) 9525;
(b) R.M. Shaltout, J.Y. Corey, N.P. Rath, J. Organomet. Chem. 513 (1995) 205.
[55] S. Mansel, U. Rief, M.-H. Prosenc, R. Kirsten, H.-H. Brintzinger, J. Organomet. Chem. 512 (1996) 225.
[56] R.W. Taft, in: M.S. Newman (Ed.), Steric Effects in Organic Chemistry, Wiley, New York, 1956, p. 556.
[57] C.K. Hancock, E.A. Meyers, B.J. Yagar, J. Am. Chem. Soc. 83 (1961) 4211.
[58] V.A. Pal'm, Fundamentals of the Quantitative Theory of Organic Reactions, Khimiya, Leningrad, 1977 (in Russian).
[59] M.J. Charton, J. Am. Chem. Soc. 91 (1969) 615.
[60] M.J. Charton, J. Am. Chem. Soc. 91 (1969) 619.
[61] N.M. Bravaya, Z.M. Dzhabieva, V.P. Maryin, V.V. Strelets, Polimery 42 (1997).
[62] A.N. Panin, O.N. Babkina, N.M. Bravaya, Russ. Chem. Bull. 49 (2000) 303.
[63] A.N. Panin, O.N. Babkina, N.M. Bravaya, Polimery 46 (2001) 44.
[64] G.L. Soloveichik, A.B. Gavrilov, V.V. Strelets, Metalloorg. Khim. 2 (1989) 431 (Organomet. Chem. USSR 2 (1989) for Engl. Transl.).
[65] M. Linnilahti, T.A. Pakkanen, Macromolecules 33 (2000) 9205.
[66] J.A. Støvneng, A. Stokvold, K. Thorshaug, E. Rytter, in: W. Kaminsky (Ed.), Metalorganic Catalysts for Synthesis and Polymerisation, Springer, 1999, p. 136.
[67] H. Wigum, K.-A. Solli, J.A. Støvneng, E. Rytter, J. Polym. Sci. A: Polym. Chem. 41 (2003) 1622.
[68] H. Wigum, L. Tagen, J.A. Støvneng, E. Rytter, J. Polym. Sci. A: Polym. Chem. 38 (2000) 3161.
[69] A. Shiga, Res. Chem. Interm. 28 (2002) 485.
[70] T. Motoki, A. Shiga, J. Comput. Chem. 25 (2004) 106.
[71] H. Katsumi, Y. Kikuzono, M. Yoshida, T. Motoki, A. Shiga, LUMMOX version 1.10, Sumitomo Chemical Co., Tokyo, 1999.
[72] W. Spaleck, M. Aulbach, B. Bachmann, F. Küber, A. Winter, Macromol. Symp. 89 (1995) 237.
[73] V. Cruz, J. Ramos, A. Muñoz-Escalona, B. Peña, J. Martinez-Salazar, Polymer 45 (2004) 2061.
[74] S.M. Green, G.R. Marshall, Trends Pharmacol. Sci. 16 (1995) 285.
[75] B.C. Taverner, J. Comput. Chem. 17 (1996) 1612.
[76] (a) M.L. Caffrey, T.L. Brown, Inorg. Chem. 30 (1991) 3907;
(b) M.-G. Choi, T.L. Brown, Inorg. Chem. 32 (1993) 5603;
(c) T.L. Brown, K.J. Lee, Coord. Chem. Rev. 128 (1993) 89;
(d) T.L. Brown, D.P. White, Inorg. Chem. 34 (1995) 2718;
(e) R.J. Bubel, W. Douglass, D.P. White, J. Comput. Chem. 21 (2000) 239.